Workshop on Visualisation in Environmental Sciences (EnvirVis) (2018)
R. Bujack and K. Rink and D. Zeckzer and S. Jänicke (Editors)

Visualizing Electrical Power Systems as Flow Fields

Samantha Molnar[1,2] and Kenny Gruchalla[1]

[1]National Renewable Energy Lab, Golden, CO USA
[2]University of Colorado Boulder, Boulder, CO USA

Abstract

We describe a method for visualizing data flows on large networks. We transform data flow on fixed networks into a vector field, which can be directly visualized using scientific flow visualization techniques. We evaluated the method on power flowing through two transmission power networks: a small, regional, IEEE test system (RTS-96) and a large national-scale system (the Eastern Interconnection). For the larger and more complex transmission system, the method illustrates features of the power flow that are not accessible when visualizing the power transmission with traditional network visualization techniques.

1. Introduction

We introduce a new technique to visualize flow on networks by constructing vector fields based on the network's flow of information. Our method allows us to use standard flow visualization techniques on large networks to highlight salient features without removing important topological information. We explore applications of our method to electric power systems, but emphasize that this technique is applicable to any complex network with information exchange.

An electrical power system is a network of components connected by lines that deliver electricity from generators to consumers. Power systems around the world are undergoing significant changes in recent years, with the addition of renewable generation sources such as wind and solar. It is crucial to understand how renewable generation sources influence power flow on the existing system so we can determine critical junctions and interactions in the system. Visualization of power flow can help maintain and increase the reliability of power systems. There are generally two categories of electric power grids: *transmission systems* which span long distances carrying high-voltage power from generators to electrical substations, and *distribution systems* which deliver power from electrical substations to individual consumers. Distribution systems typically have a radial topology forming acyclic connected graphs, while transmission systems tend to have much more complex interconnected networks forming cyclic non-planar graphs. At a given instant in time, these networks can be considered directed graphs with some magnitude of power flowing from one vertex along an edge to another vertex. The magnitude and direction of power flowing on these graphs is dynamic, varying in time. The topology of these graphs can change with the operation of circuit breakers or switches; however, these are relatively rare events. For our investigation, we are only concerned with the dynamics of the flow not the topology.

We evaluate our visualization approach on power flowing through two transmission power networks: a small IEEE test system (RTS-96) and a large system (the Eastern Interconnection). The small test system is simple enough to use traditional visualization techniques, allowing us to determine if the vector field represents the power flow accurately. The Eastern Interconnection provides a real-world test case that is too complex for existing visualization techniques to convey the flow trends (see Figure 1).

There are documented needs to visualize general trends of flow on complex network structures; for example, the flow of information on biological networks [AKK*10] and neural networks [LSKK16], and the flow of power on electrical networks [CK15] are compelling examples. Most techniques involve representing the flow explicitly on line graphs with glyphs (e.g., arrows) and line attributes (e.g., color and width) [OW00b]. These techniques are often sufficient for small networks but are inefficient or unreadable for larger networks.

To visualize large-scale networks some form of aggregation becomes neccessary. Two common approaches are chord diagrams and edge bundling. A chord diagram represents directed interrelationships between groups of objects, where these objects are arranged along a circle and connected with Beźier curves [KSB*09]. Chord diagrams can be used to represent data flow on a directed graph [GNB16] by grouping vertices into regions and representing the net flow between regions in the chord diagram. The chord diagram provides a quantitative view of net flow, but abstracts that flow away from the toplogy of the network. Edge bundling is a technique to simplify a graph by spatailly grouping similar graph edges, decluttering and revealing underlying structure in large networks [LHT17]. However, large transmission networks, like the Eastern Inconnection, have dense multi-scale mesh-like topologies that provide few similar graph edges for edge bundling to a group. For example, we applied geometry based edge bundling

DOI: 10.2312/envirvis.20181139

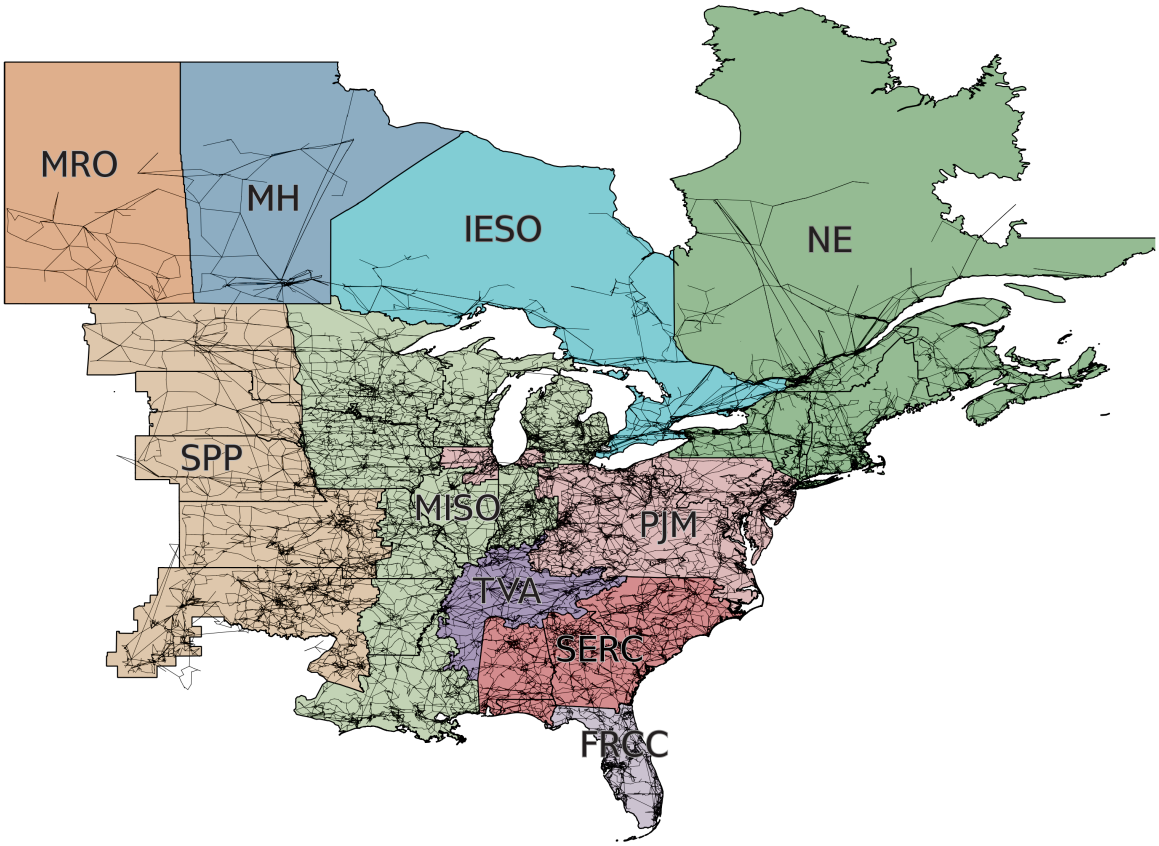

Figure 1: *A model of the Eastern Interconnection transmission network presents a visualization challenge with flows across 70,000 transmission lines. The labeled areas indicate independent system operators controlling power in those regions. We would like to understand* ***how*** *and* ***where*** *these areas exchange power.*

(GBEB) [CZQ*08] to the Eastern Interconnection. GBEB bundles edges based on a kernel density estimation of the primary edge directions. As seen in Figure 2, this method does well with edges in the North East coming from Canada to the United States, but it fails to declutter the majority of the Eastern Interconnection. This is because the power system is mainly composed of star-like motifs that come to a single node from various directions. We also applied kernel density edge bundling (KDEB) [HET12], which is the base algorithm for other edge bundling techniques that use edge attributes as an indicator for bundling [PHT15]. KDEB determines the density of edges, computes the gradient of this density, and iteratively moves edges in the direction of the gradient to bundle edges. Figure 3 shows KDEB applied to the Eastern Interconnection, and while more edges are bundled than the GBEB approach, it does little to alleviate the clutter of the network. Although the network is dense, this is generally uniformly distributed over space. Furthermore, many of the edges that are close together in the topology do not have a uniform direction, which makes it unclear how and in what direction they should be bundled. The conclusion we can draw from applying these edge bundling techniques is that due to the mesh-like structure of the Eastern Interconnection, there is little advantage to bundling the edges of the network to try and reduce visual clutter and obtain useful information about power flow across the network. An alternate approach is required to understand power flow across the network.

Our technique does not visualize aggregated edges, but instead visualizes aggregated *flow* across the network. We can find no description in the literature of transforming the flow across a complex network into a vector field for the visualization of flow trends. Lobov et al. [LSKK16] appear to use a similar technique to understand properties of neural networks in response to a stimulus; however, their technique is not well documented, and it is unclear how they form their vector field. Nevertheless, this provides an excellent example of the need to further analyze parameter choices for

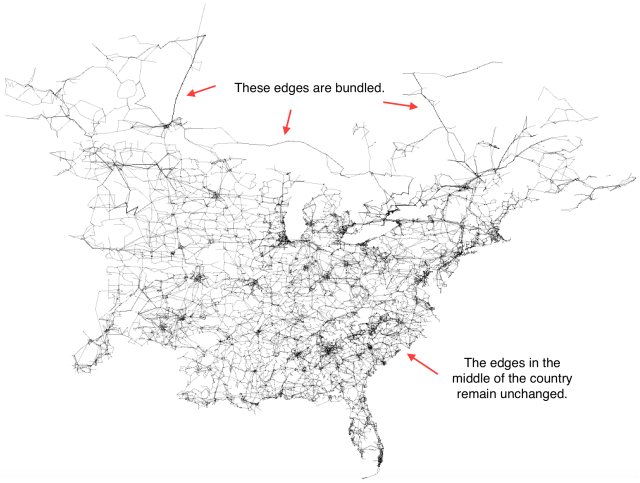

Figure 2: *The result of geometry based edge clustering on the Eastern Interconnection [CZQ*08]. Most of the network remains unbundled. Long transmission lines coming from Canada are bundled using this technique, but small star-like motifs in the South Eastern United States are mostly untouched.*

Figure 3: *The result of kernel density edge bundling on the Eastern Interconnection [HET12]. Longer transmission lines are moved towards denser parts of the network due to the edge bundling formulation. Since power systems consist of either small lines densely connected together with little overlap, or long lines that, edge bundling techniques are an ill suited visualization technique.*

this type of visualization in order to understand how these choices affect analysis results.

Our method allows us to use standard flow visualization techniques on large networks to highlight salient features without removing important topological information. Furthermore, we will show that insightful knowledge of power exchange on the system can be obtained using our visualization technique.

2. Methods

We analyze general flow patterns across a network by creating a vector field based on the network dynamics and topology. Let the network in question be represented by G with V vertices and E edges. We take each directed edge $e_{i,j} \in E$ which connects nodes $i, j \in V$ and form a vector, $\hat{e}_{i,j}$, based on its location in space. Each $\hat{e}_{i,j}$ has an associated flow, $f_{i,j}$. To begin constructing the vector field, we place the network in an $n \times n$ square mesh M. Each cell in the mesh, $m_{l,k} \in M$, where l defines the row and k defines the column, will contain a vector. The function that computes this vector is shown in Equation 1.

$$V_{total}(l,k,p,\sigma) = V_{flow}(l,k) + V_{grad}(l,k,\sigma) + V_{kern}(l,k,p) \quad (1)$$

Where V_{flow} is the vector sum of all edge flows through a cell, V_{grad} is the gradient of a Gaussian convolution to attract the flow towards the topology, and V_{kern} is a Gaussian weighting of nearby cells.

2.1. Calculating V_{flow}

V_{flow} represents the flow of information on the network. For each cell in the grid that contains $\hat{e}$, we compute the sum of the vector flows, defined by Equation 2.

$$V_{flow}(l,k) = \sum_{s=0}^{s=|E|} \delta(\hat{e}_s, m_{l,k}) * (f_s \hat{e}_s) \quad (2)$$

$$\delta(\hat{e}_s, m_{l,k}) = \begin{cases} \hat{e}_s \in m_{l,k} & 1 \\ otherwise & 0 \end{cases}$$

A depiction of V_{flow} of the RTS-96 system is shown in Figure 4a. Notice that very few of the cells in the mesh are filled with non-zero vectors. This will cause problems for traditional flow techniques that seed streamlines or path lines at random positions. There is also little guarantee that flow lines seeded at node positions will remain in the flow field without other forces pushing it back into this area. For these reasons, we add a gradient force to the vector field.

2.2. Calculating V_{grad}

The purpose of V_{grad} is to fill cells that do not directly intersect the network with vectors that point towards the topology of the network. This would allow streamlines seeded away from the network topology to converge toward the network topology. If we imagine placing the network on a rubber sheet, we would see the sheet sink down where the lines are, and balls rolling on the sheet would tend to fall into the valleys, or the edges of the network (see Figure 4b).

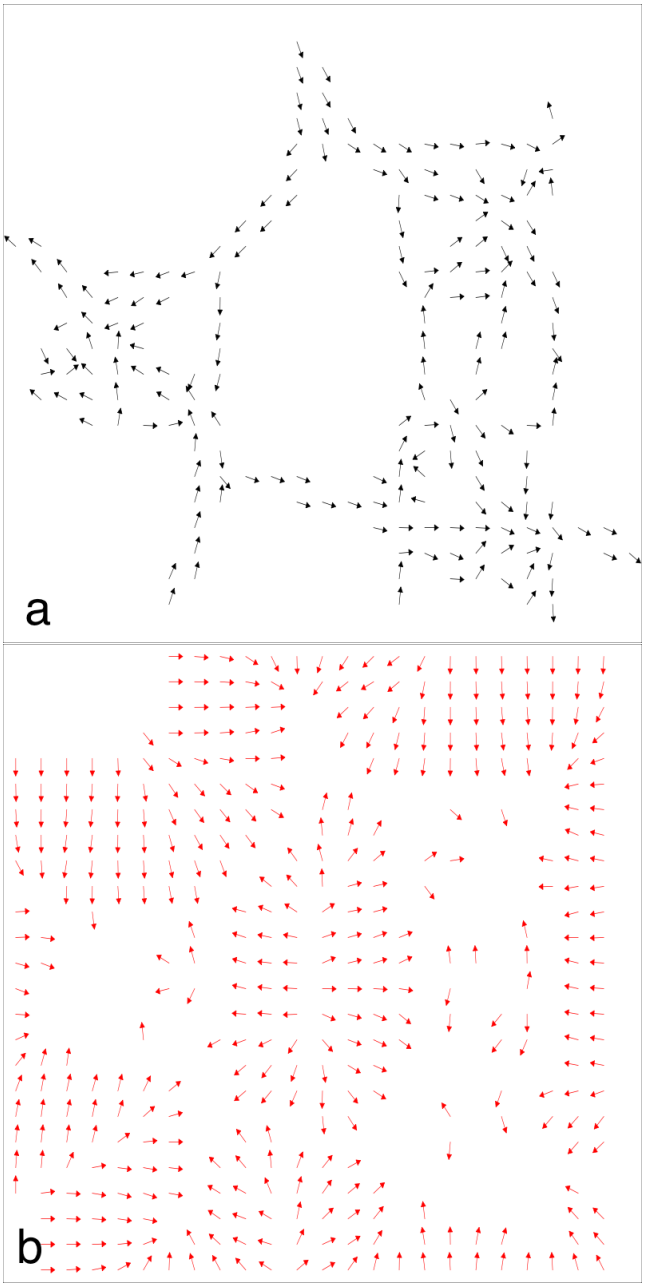

Figure 4: *Vector field representation of the RTS-96 test system with a 25×25 grid.* ***a)*** *directly represents the flow on the network by encoding V_{flow}.* ***b)*** *V_{grad} directs flow back towards the topology of the network.*

To achieve this effect we first calculate the weighted sum of each cell in the network, where the weight represents how much of each edge in E the cell contains. We traverse each edge, $e_{i,j}$, in unit vector intervals, and for each step we compute which cell $m_{l,k}$ is closest to the current position and add 1 to that cell's weight $w_{l,k}$ in the matrix W. We then compute V_{grad} based on Equation 3.

$$V_{grad}(l,k,\sigma) = \nabla \frac{1}{2\pi\sigma^2} e^{-\frac{w_{l,k}}{2\sigma^2}} \tag{3}$$

The only tunable parameter in V_{grad} that we explore in this work is σ which, in our metaphor, represents how fast flow moves towards the edges of G. As σ increases, the number of cells with a non-zero vector decreases.

2.3. Calculating $V_{kern}(l,k,p)$

Finally, in order to make the vector field less abrupt at the boundary of cells that contain network edges and cells that do not, we add a small vector to each cell that is the average of its neighbors. For example, if $\sigma = 1$, then V_{grad} points cells without flow directly towards the topology, exhibited in Figure 5a. $V_{kern}(l,k,p)$ smooths this transition and slightly points cells without edges towards the majority direction of its neighbors, shown in Figure 5b. In Equation 4, p represents the size of the neighborhood we average over; $p = 1$ represents the surrounding ring of neighbors around a cell (of which there are at most 8), then $p = 2$ represents the next surrounding ring and so on. The function $g(p)$ is a gaussian function that determines how much weight each neighbor cell contributes to the average. In this paper, we focus on varying p to understand how the size of a neighborhood changes the vector field rather than changing the weight of the contribution from the neighborhood.

$$V_{kern}(l,k,p) = \sum_{s=l-p}^{l+p} \sum_{r=k-p}^{k+p} g(p)(V_{flow}(s,r) + V_{grad}(s,r)) \tag{4}$$

The parameter space for $V_{total}(l,k,p,\sigma)$ is large and various inputs can change the types of conclusions one could draw about the network flow. In the following section we will explore how various inputs of V_{total} change the observed flow dynamics on two power system test cases.

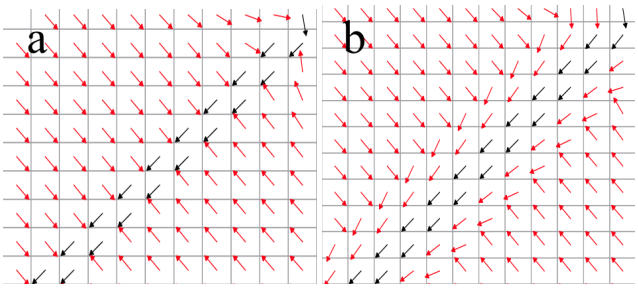

Figure 5: *A graph edge represented as a vector field. Black vectors indicate cells that contain an edge with flow and red vectors indicate cells that do not.* ***a)*** *is constructed without $V_{kern}(l,k,p)$ and* ***b)*** *is constructed with $V_{kern}(l,k,p)$ and $p = 1$.*

3. Experimental Results - Electric Power Systems

There are few techniques for the visualization of power systems data [MJC12]. The simple one-line diagram, a static diagram with single lines and schematic symbols to indicate the path and components on an electric circuit [vM06], is a standard representation for the static structure of the system. Most visualization research has focused on augmenting the one-line diagram with flow data. Various researchers [MC93, LQ98] have proposed encoding electrical flow as line width and color and including arrows for flow direction. Two-dimensional contours have been used to visualize network data [WO00, OW00b], market data [OW00a], and system stability margins [OKW99, KW02]. However, these techniques do not scale to large transmission systems with tens of thousands of lines. The visualization of large transmission networks more typically aggregate the line flows to the net flow or *interchange* between regions of the network. These aggregated flows have been represented as ribbons in a chord diagram [GNB16] (see Figure 6). Net interchange visualizations provide critical information on power transfer between large regions in aggregate but fail to show how that interchange occurs. For example, in Figure 6 we see ≈3 GW of power flowing from SERC to TVA, and ≈3 GW of power flowing from TVA to PJM. But we do not know where along that interconnection this exchange occurs. Furthermore, we can speculate that some of the flow from SERC to TVA is transferred to PJM, but we cannot decisively know this based on the chord diagram. Additional locational information could be useful to determine where additional transmission lines should go, which transmission lines are under stress at various times, and potentially change market exchange calculations.

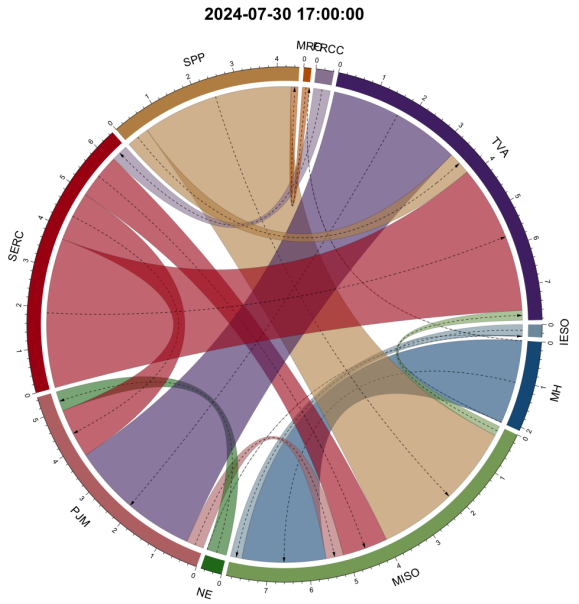

Figure 6: *A chord diagram of a time step of the Eastern Renewable Generation Integration Study (ERGIS). Large transmission networks have tens of thousands of lines, directly visualizing these lines is impractical. Transmission studies such as ERGIS have resorted to only visualizing aggregated flow between regions. There is significant flow between SERC and TVA, and TVA to PJM, but it is unclear if the flow from SERC to TVA is then going to PJM.*

3.1. RTS-96 System – Validation Case

IEEE RTS-96 [GWA*99] is a test system commonly used in transmission power system reliability studies. The system is a cyclic non-planar graph with 73 vertices connected by 120 edges comprised of three subnetworks. RTS-96 is small enough to directly visualize flows on the network with arrow glyphs indicating direction and line properties (e.g., color, width) representing flow magnitude (see Figure 7). Clearly, a system this small is best represented with these traditional techniques. We apply our method to RTS to evaluate if our vector field construction represents the power flow consistently.

We depict these vector fields using streamlines, but other vector field visualization techniques (i.e., path lines and line interval convolution) are directly applicable. To evaluate the correctness of the constructed vector field, we systematically seeded stream lines near sources (i.e., buses with electrical generation) on RTS-96 and followed those stream lines to the sinks (i.e., nodes with electrical loads). The streamlines do travel from sources to sinks on paths that generally follow the network (see Figure 8a and b). However, how closely they follow the network depends on the parameters of the vector field construction. A significant flow difference can be observed between Figure 8a and Figure 8b at the location of the bottom orange seed area. The final destination of the streamlines changes from one node to another. Since Figure 8b has a larger neighborhood and based on the direction the streamlines originate from, they go towards the bottom right nodes instead of the farthest right node. We explore the vector field construction parameters n, p, and σ on the RTS-96 system (a subset of that investigation is shown in Figure 9). First, as the grid size n becomes larger (and the cells smaller), the network topology becomes more defined in the vector field, as there is less aggregation per cell. For example, compare $n = 100$ in Figure 9a and $n = 1000$ in Figure 9d. When there are fewer cells, the larger flows dominate the vector space and show more of the cumulative dynamics on the system. When there are more cells, many of the smaller flows are captured. In areas where a cell contains an intersection, the constructed field will push flow in the aggregate direction of all edges in that cell weighted by their magnitude. Second, as we increase σ relative to the grid size, the number of cells with non-zero vectors increases and stream lines can be seeded farther away from the network. Although, the stream lines converge to the network, the visual features created as σ increases may be difficult to interpret. For example, in Figure 9c a saddle has formed in the middle of the network that could be misconstrued as a pathway in the network. This feature occurs because σ has become large enough compared to the grid size to fill cells in the very center of the network. Based on V_{grad} cells to the right of the saddle point towards the right part of the network and cells to the left of the saddle point towards the left of the network. Understanding how domain experts might interpret these flow patterns will be necessary and is a topic for future work. But with proper parameter selection, many of these artifacts are avoidable. Finally,

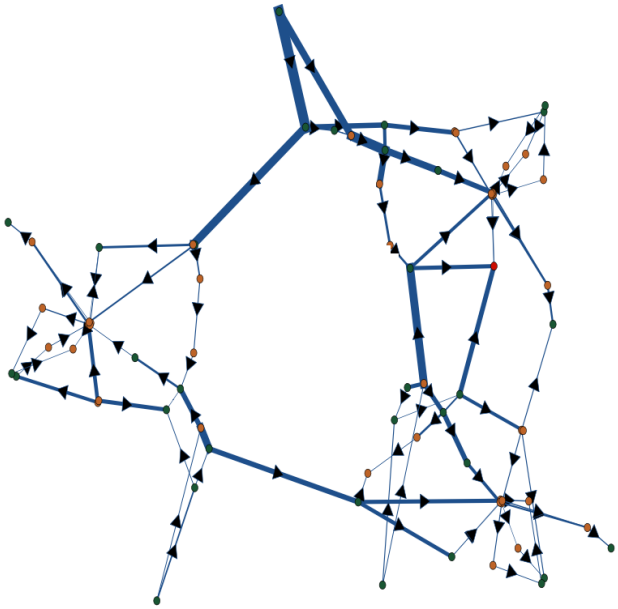

Figure 7: *RTS-96 topology with line widths representing power magnitude and arrows indicating direction. Generator buses (i.e., sources) are colored green, load buses (i.e. sinks) are colored orange, and the swing bus is colored red.*

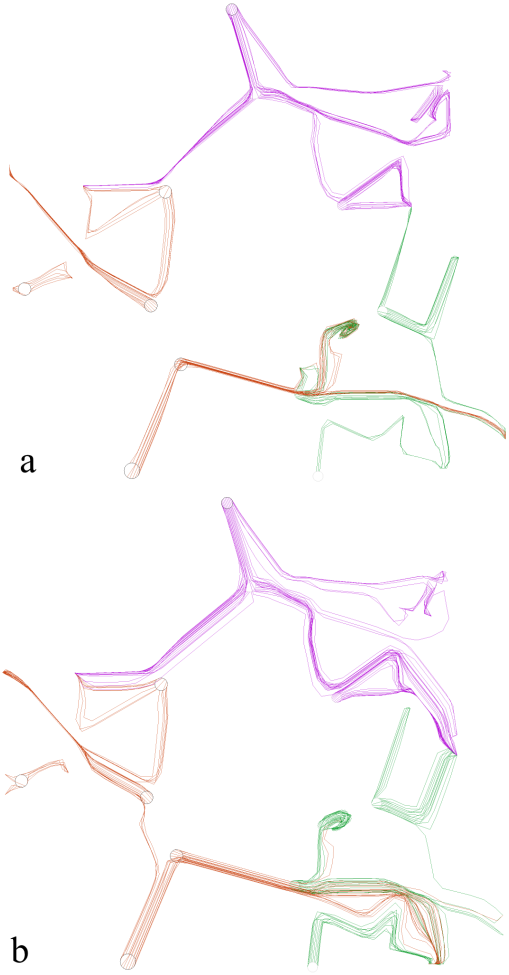

Figure 8: ***a and b)*** *Streamlines seeded near generators generally follow the network path to the system's loads center. How the stream lines follow the network path is impacted by the construction parameters. Colors are based on which area the streamlines originate from, area 1 is purple, area 2 is orange and area 3 is green. The images were both constructed with* $n = 1000$ *and* $\sigma = 1$ *and vary in kernel width a)* $p = 10$ *b)* $p = 20$.

the number of neighbors considered in V_{kern} changes how much influence larger flow magnitudes have on the direction of the overall flow. We find that a smaller neighborhood stays closer to the true topology of the system, while large neighborhoods provide clear illustrations of the cumulative flow. The choice for this parameter is dependent on how much aggregation one wishes to show in the visualization.

There is one notable artifact visible in RTS-96 for all of the streamlines shown in Figure 9, a spiral sink occurs in the lower right hand area. This feature forms in a non-planar area of the network, where lines in the network cross but do not intersect in the actual physical topology (i.e., they are not connected by a node). While there is a sink located in the vicinity, the intersection of an edge close to this sink causes a spiraling effect where there in fact is none. Our treatment of edge crossings is beneficial if one wishes to observe the general flow trend in the network, but it may not give an accurate depiction of small-scale flow features. As the mesh grid becomes finer, this effect is less obvious because the cell containing the intersection plays a much smaller role in the overall vector field which provides a more detailed view of the flow.

3.2. ERGIS System – Motivating Case

The Eastern Interconnection is the largest power system in North America and one of the most complex power systems in the world. We applied our visualization technique to data from the Eastern Renewable Generation Integration Study (ERGIS) [BTP*16] that models the Eastern Interconnection with over 70,000 transmission lines. This network provides a real-world test case for our visualization technique, where directly rendering the line flows is impractical. We compared the aggregated flow visualization from the study, which shows us how much net power flows between the regions, to our results (see Figure 10). In general, the path of the stream lines are confirmed by the chord diagram. For example, there is significant flow between SERC and TVA and between SPP and MISO (reference Figure 1 for region labeling). While the chord diagram provides a quantitative measure of the net interchange, the streamlines provide more qualitative detail to where along the interface that interchange is occurring. We can gain more insight into the flow characteristics by isolating the streamline seeding in particular regions and analyzing their path. Figure 11 shows flow be-

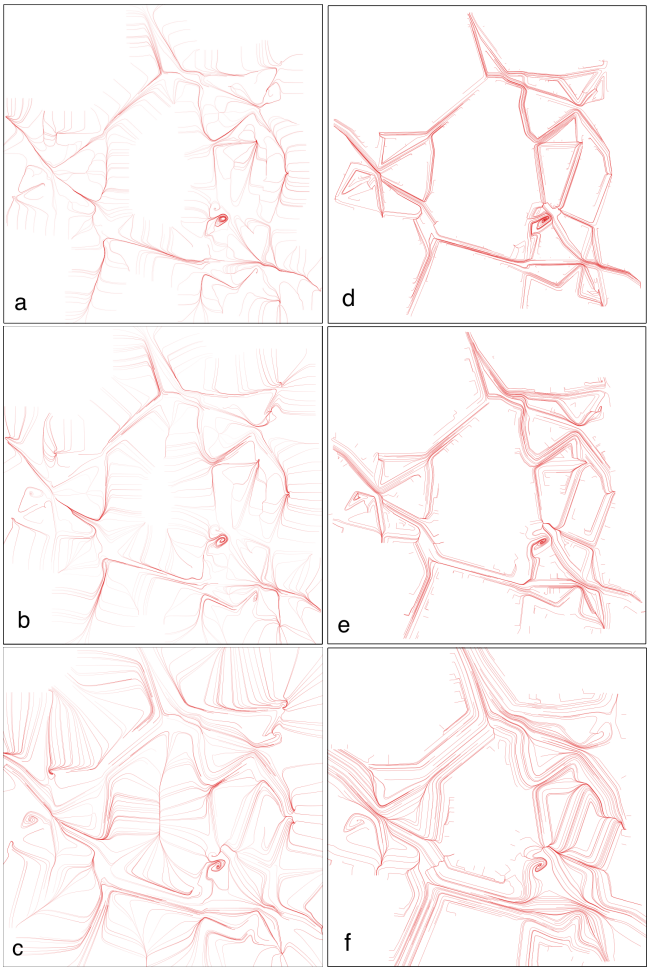

Figure 9: *Streamlines of various inputs for RTS-96 vector field where the left column has $n = 100$ and the right column has $n = 1000$. **a)** $p = 1$, $\sigma = 1$ **b)** $p = 1$, $\sigma = 2$ **c)** $p = 4$, $\sigma = 4$ **d)** $p = 10$, $\sigma = 1$ **e)** $p = 10$, $\sigma = 2$ **f)** $p = 40$, $\sigma = 4$. We scale the neighborhoods for the different grid sizes so that they represent the same amount of space, and all of the vector fields use $g(p) = .05e^{-\frac{p-1}{200}}$. Animated version here.*

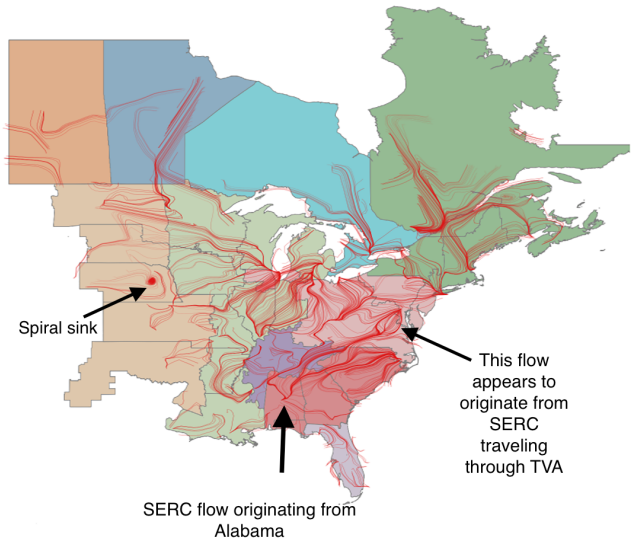

Figure 10: *Streamlines, distributed proportionally to the vector magnitude, showing detailed flow of power for the Eastern Interconnection ($n = 1000$, $\sigma = 1$, $p = 10$). Large amounts of power is flowing in to the mid-west region.*

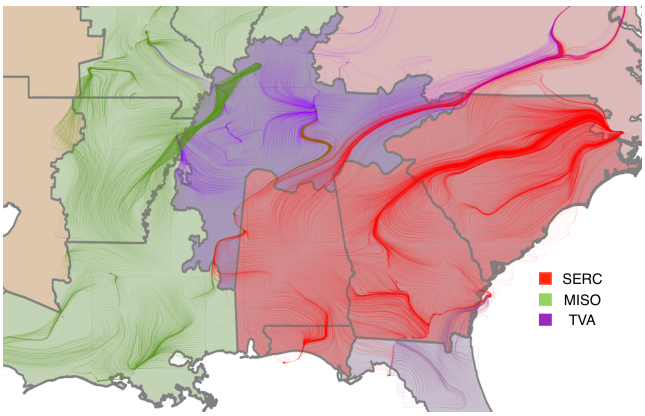

Figure 11: *Streamlines colored based on which region they originated from. Flows originating from SERC traveling through TVA into PJM are clearly visible. Likewise bi-directional flow can be seen between TVA and MISO.*

tween different areas in the Eastern Interconnection. Based on the aggregate flow in the chord diagram (Figure 6), we know that a significant amount of power flows from SERC to TVA, and from TVA to PJM. However, what we can now see from Figure 11 is that a significant amount of power that flows from SERC to TVA then flows to PJM. Most of that SERC-TVA flow originates in Alabama and not elsewhere in the region. Additionally, we can see bi-directional flow between MISO and TVA; although, in Figure 6 we are only privy to relatively small net interchange coming in to TVA from MISO. This is new directional information that we could only speculate based on the original visualizations. Preliminary examination of these results with domain scientists indicate that this novel vector field construction provides useful locational information that can be used during development, testing, and analysis of power flow models and simulations.

The vector field construction parameters have a similar effect on the large-scale system as they did on the small test system. Denser meshes better resolve individual transmission lines, while larger kernel sizes provide more aggregated versions of the flow. A spi-

raling sink artifact, like the one apparent in RTS-96, can also be found in our Eastern Interconnection construction in eastern Nebraska (see Figure 10). Like RTS-96, there appears to be a non-planar cluster of transmission lines in this area of Nebraska. In all likelihood, this is an artifact of the construction, but with alternate parameters this artifact does disappear.

4. Conclusions and Future Work

We introduced a method for visualizing data flows on large networks by transforming those flows into a vector field. The method clearly shows promise. On our small-scale test case we verified that the technique represents the predominate flow features. On our large-scale test case we were able to identify complex flow exchanges between different areas of the Eastern Interconnection transmission system. We have a better understanding of how power flows between regions with our visualization than an aggregate view can present and a traditional line glyph rendering cannot handle.

However, the method has some limitations. The construction captures the most dominate flows at the expense of averaging out the details of the flows. More concerning, non-planar areas of the graph can lead to spiraling sink artifacts. A more sophisticated vector field allowing for probabilistic and/or conditional cells could improve these situations. Developing these multi-state cells and the visualization algorithms to support them is left for future work.

Our parameter investigation indicates that larger grid sizes yields more accurate flow information while larger neighborhoods causes larger flow magnitudes to dominate more of the vector space. Future work will extend the investigation to time-varying vector field visualization methods so we can understand how flow evolves on a network over time. User studies will be necessary to understand how domain experts interpret the flow visualizations in relation to the flow on the underlying network, which may provide a mechanism to better tune the parameters of the construction.

5. Acknowledgements

This work was supported by the U.S. Department of Energy under Contract No. DE-AC36-08GO28308 with Alliance for Sustainable Energy, LLC, the Manager and Operator of the National Renewable Energy Laboratory. Funding provided by U.S. Department of Energy Office of Energy Efficiency and Renewable Energy. NREL is a national laboratory of the U.S. Department of Energy, Office of Energy Efficiency and Renewable Energy, operated by the Alliance for Sustainable Energy, LLC. The U.S. Government retains and the publisher, by accepting the article for publication, acknowledges that the U.S. Government retains a nonexclusive, paid-up, irrevocable, worldwide license to publish or reproduce the published form of this work, or allow others to do so, for U.S. Government purposes. The authors would like to thank Nicholas Brunhart-Lupo and Kristi Potter for useful conversations and insight on this work. We would also like to thank Aaron Bloom and Clayton Barrows for preliminary examination of the results.

References

[AKK*10] ALBRECHT M., KERREN A., KLEIN K., KOHLBACHER O., MUTZEL P., PAUL W., SCHREIBER F., WYBROW M.: *On Open Problems in Biological Network Visualization*. Springer Berlin Heidelberg, Berlin, Heidelberg, 2010, pp. 256–267. doi:10.1007/978-3-642-11805-0_25. 1

[BTP*16] BLOOM A., TOWNSEND A., PALCHAK D., NOVACHECK J., KING J., BARROWS C., IBANEZ E., OÃĆÂĆÑÂĎćCONNELL M., JORDAN G., ROBERTS B., DRAXL C., GRUCHALLA1 K.: *Eastern Renewable Generation Integration Study*. Tech. Rep. NREL/TP-6A20-64472, National Renewable Energy Laboratory, August 2016. 6

[CK15] CUFFE P., KEANE A.: Visualizing the electrical structure of power systems. *Systems Journal, IEEE PP*, 99 (2015), 1–12. doi:10.1109/JSYST.2015.2427994. 1

[CZQ*08] CUI W., ZHOU H., QU H., WONG P. C., LI X.: Geometry-based edge clustering for graph visualization. *IEEE Transactions on Visualization and Computer Graphics Volume 14, Issue 6* (October 2008), 1277–1284. URL: https://www.microsoft.com/en-us/research/publication/geometry-based-edge-clustering-graph-visualization/. 2, 3

[GNB16] GRUCHALLA K., NOVACHECH J., BLOOM A.: Visualization of the eastern renewable generation integration study. In *Proceedings of the International Conference for High Performance Computing, Networking, Storage and Analysis* (2016), SC '16, ACM. 1, 5

[GWA*99] GRIGG C., WONG P., ALBRECHT P., ALLAN R., BHAVARAJU M., BILLINTON R., CHEN Q., FONG C., HADDAD S., KURUGANTY S., LI W., MUKERJI R., PATTON D., RAU N., REPPEN D., SCHNEIDER A., SHAHIDEHPOUR M., SINGH C.: The ieee reliability test system-1996. a report prepared by the reliability test system task force of the application of probability methods subcommittee. *IEEE Transactions on Power Systems 14*, 3 (Aug 1999), 1010–1020. doi:10.1109/59.780914. 5

[HET12] HURTER C., ERSOY O., TELEA A.: Graph bundling by kernel density estimation. *Comput. Graph. Forum 31*, 3pt1 (June 2012), 865–874. URL: http://dx.doi.org/10.1111/j.1467-8659.2012.03079.x, doi:10.1111/j.1467-8659.2012.03079.x. 2, 3

[KSB*09] KRZYWINSKI M. I., SCHEIN J. E., BIROL I., CONNORS J., GASCOYNE R., HORSMAN D., JONES S. J., MARRA M. A.: Circos: An information aesthetic for comparative genomics. *Genome Research* (2009). doi:10.1101/gr.092759.109. 1

[KW02] KLUMP R. P., WEBER J. D.: Real-time data retrieval and new visualization techniques for the energy industry. In *Proceedings of the 35th Annual Hawaii International Conference on System Sciences, 2002. HICSS* (Jan. 2002), pp. 712–717. doi:10.1109/HICSS.2002.993964. 5

[LHT17] LHUILLIER A., HURTER C., TELEA A.: State of the art in edge and trail bundling techniques. *Comput. Graph. Forum 36*, 3 (June 2017), 619–645. URL: https://doi.org/10.1111/cgf.13213, doi:10.1111/cgf.13213. 1

[LQ98] LIU Y., QIU J.: Visualization of power system static security assessment based on gis. In *Power System Technology, 1998. Proceedings. POWERCON '98. 1998 International Conference on* (Aug 1998), vol. 2, pp. 1266–1270 vol.2. doi:10.1109/ICPST.1998.729289. 5

[LSKK16] LOBOV S., SIMONOV A., KASTALSKIY I., KAZANTSEV V.: Network response synchronization enhanced by synaptic plasticity. *The European Physical Journal Special Topics 225*, 1 (2016), 29–39. URL: http://dx.doi.org/10.1140/epjst/e2016-02614-y, doi:10.1140/epjst/e2016-02614-y. 1, 2

[MC93] MAHADEV P., CHRISTIE R.: Envisioning power system data: concepts and a prototype system state representation. *Power Systems, IEEE Transactions on 8*, 3 (Aug 1993), 1084–1090. doi:10.1109/59.260890. 5

[MJC12] MIKKELSEN C., JOHANSSON J., COOPER M.: Visualization of power system data on situation overview displays. In *Information Visualisation (IV), 2012 16th International Conference on* (July 2012), pp. 188–197. doi:10.1109/IV.2012.41. 5

[OKW99] OVERBYE T., KLUMP R., WEBER J.: A virtual environment for interactive visualization of power system economic and security information. In *Power Engineering Society Summer Meeting, 1999. IEEE* (1999), vol. 2, pp. 846–851 vol.2. doi:10.1109/PESS.1999.787428. 5

[OW00a] OVERBYE T., WEBER J.: New methods for the visualization of electric power system information. In *Information Visualization, 2000. InfoVis 2000. IEEE Symposium on* (2000), pp. 131–16c. doi:10.1109/INFVIS.2000.885101. 5

[OW00b] OVERBYE T., WEBER J.: Visualization of power system data. In *System Sciences, 2000. Proceedings of the 33rd Annual Hawaii International Conference on* (Jan 2000), pp. 7 pp.–. doi:10.1109/HICSS.2000.926744. 1, 5

[PHT15] PEYSAKHOVICH V., HURTER C., TELEA A.: Attribute-driven edge bundling for general graphs with applications in trail analysis. *IEEE Visualization Symposium (PacificVis)* (April 2015), 39–46. URL: http://dx.doi.org/10.1109/PACIFICVIS.2015.7156354, doi:110.1109/PACIFICVIS.2015.7156354. 2

[vM06] VON MEIER A.: *Electric Power Systems: A conceptual Introduction*, first ed. Wiley-IEEE Press, 2006. 5

[WO00] WEBER J., OVERBYE T.: Voltage contours for power system visualization. *Power Systems, IEEE Transactions on 15*, 1 (Feb 2000), 404–409. doi:10.1109/59.852151. 5